

Self-Gated Fat-Suppressed Cardiac Cine MRI

R Reeve Ingle¹, Juan M Santos², William R Overall², Bob S Hu^{1,3}, and Dwight G Nishimura¹

¹Electrical Engineering, Stanford University, Stanford, California, United States, ²HeartVista, Inc., Menlo Park, California, United States, ³Palo Alto Medical Foundation, Palo Alto, California, United States

Target Audience MR physicists and clinicians interested in pulse sequence design, image reconstruction, cardiac imaging, and ventricular function.

Purpose MR cardiac cine imaging with balanced steady-state free precession (bSSFP) is commonly used to assess ventricular function. Retrospective electrocardiogram (ECG) gating is typically used to sort or interpolate the acquired data into different cardiac phases. Because the ECG signal can be corrupted by RF interference and the magnetohydrodynamic effect, self-gated approaches have been developed to derive cardiac phase information directly from acquired MR data^[1-2]. Another drawback of the standard bSSFP acquisition is the bright signal from fat, which can lead to unwanted partial-volume effects and motion artifacts. To achieve fat-suppressed steady-state contrast, an alternating repetition time (ATR) SSFP sequence was proposed for cine imaging^[3]. In this work, we develop a self-gated fat-suppressed ATR-SSFP cine imaging sequence and compare it with ECG-gated bSSFP and ATR-SSFP acquisitions.

Methods Our approach was inspired by a wideband-SSFP technique developed by Lee, *et al.*, in which the k -space center point was acquired during the unused short TR (TR_2) and used for respiratory gating^[4]. To achieve fat suppression at 1.5 T, TR_2 of ATR-SSFP is significantly shorter than that of wideband SSFP (1.15 ms vs. 2.4 ms)^[5]. By bridging the slice-select rephaser gradients of an ATR-SSFP pulse sequence, we enabled the acquisition of a 36-point 1D projection navigator during the unused TR_2 interval (Fig. 1).

Navigators were acquired every TR and used to determine cardiac phase information during breath-held cardiac cine scans. Navigators were processed using a principal component analysis (PCA) technique^[6-7], in which the complex k -space data (Fig. 2a) from all coils were stacked to form a 2D k - t matrix, and then singular value decomposition was used to compute the first right singular vector (RSV). The RSV reflects the periodic changes in the navigator signals (both magnitude and phase) and correlates very well with the cardiac cycle. The RSV was bandpass filtered (passband = 0.7-10 Hz), and then a short-time autocorrelation pattern matching technique was used to extract cardiac trigger points (Fig. 2b) for self-gated cine reconstruction.

In-vivo ATR-SSFP and bSSFP scans were performed on a GE 1.5 T scanner using the RTHawk real-time environment^[8] (HeartVista, Inc., CA) and an 8-channel cardiac receive array. A 2DFT readout and linear k -space segmentation with 12 views per segment (58-ms temporal resolution) were used with the following parameters: $FOV=30\times30\text{ cm}^2$, $res.=1.5\times1.9\text{ mm}^2$, flip angle = 50°, slice thickness = 6 mm, $TR_1/TR_2 = 3.65/1.15$ ms, scan duration = 14–21 s, 500 dummy views. To sample the entire RR interval, each k -space segment was repeated for a duration spanning 1.15 times the expected RR interval. Acquired k -space views were retrospectively sorted based on the times from the recorded ECG R-wave or self-gating trigger points, and linear interpolation was used to reconstruct images at 30 cardiac phases. A total of 9 healthy volunteers and 5 patients were scanned using short-axis (SA), 4-chamber (4CH), 3-chamber (3CH), and 2-chamber (2CH) scan planes to compare the self-gating and ECG-gating techniques.

Results Figure 2b shows the filtered self-gating signal from a volunteer scan, with ECG and navigator-derived trigger points indicated. The trigger delay (difference of ECG and navigator trigger times^[2]) has a non-zero mean (218 ms), reflecting navigator triggering during a different part of the cardiac cycle. More importantly, the trigger variance (standard deviation of trigger delay^[2]) is small (6.8 ms), reflecting little variation in trigger times between the two methods. Among the 9 volunteer and 5 patient studies (61 breath-held scans), the mean trigger variance was 13 ms (SA), 23 ms (4CH), 24 ms (3CH), and 29 ms (2CH). Figure 3 shows diastolic and systolic SA and 3CH ATR-SSFP images reconstructed using ECG gating and self gating, as well as difference images scaled by 10x. Figure 4 compares the same basal SA slice from a self-gated ATR-SSFP scan and an ECG-gated bSSFP scan with matched parameters and $TR=3.6$ ms.

Discussion & Conclusion Preliminary results in volunteers and patients suggest that images reconstructed with the proposed self-gating technique agree favorably with standard ECG gating. The mean trigger variance was smaller for SA scans, in which the primary flow direction is through-plane, aligned with the navigator readout axis and perpendicular to the flow-sensitive phase-encode axis. The ATR-SSFP sequence achieved good fat suppression around the heart (Fig. 4). Compared to bSSFP, partial volume effects that cause fat-water cancellation (e.g., coronary arteries, Fig. 4) were significantly reduced with the ATR-SSFP sequence. In conclusion, the proposed self-gated ATR-SSFP sequence has enabled robust fat-suppressed cine imaging without the need for external ECG gating.

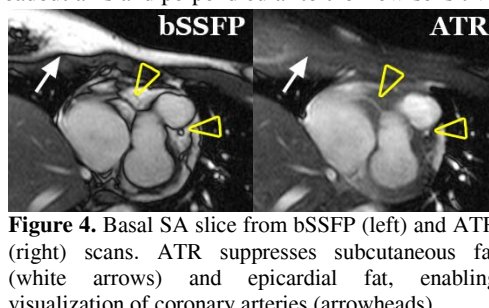


Figure 4. Basal SA slice from bSSFP (left) and ATR (right) scans. ATR suppresses subcutaneous fat (white arrows) and epicardial fat, enabling visualization of coronary arteries (arrowheads).

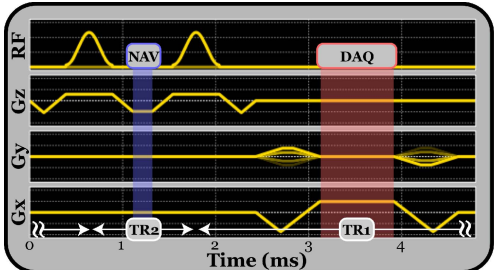


Figure 1. Navigated ATR-SSFP pulse sequence. Bridging slice-select rephasing lobes during TR_2 enables acquisition of 1D navigators along k_z .

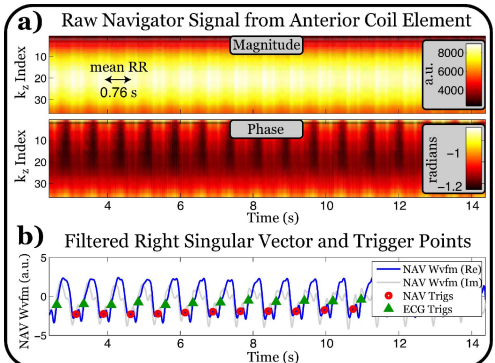


Figure 2. Navigator signals. **(a)** Raw navigator k -space data from a single anterior coil element shows periodic fluctuation with the cardiac cycle. **(b)** PCA and bandpass filtering yield a self-gating signal that is used to derive cardiac trigger points (red circles). Navigator trigger spacing agrees well with measured ECG triggers (green triangles).

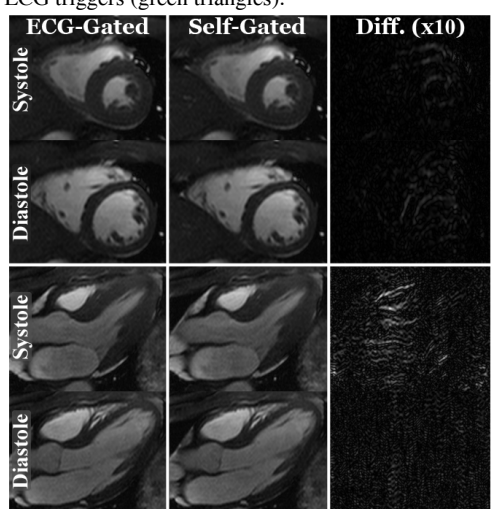


Figure 3. SA (top) and 3CH (bottom) images reconstructed with ECG-gating (left) and self-gated (middle). Difference images (right) show little difference between the two reconstructions.

References

- [1] Spraggins TA, *MRI* 8:675-81, 1990.
- [2] Larson AC, *et al.*, *MRM* 51:93-102, 2004.
- [3] Lin HY, *et al.*, *JCMR* 10:22, 2008.
- [4] Lee HL, *et al.*, *Proc 17th ISMRM*, p. 4643, 2009.
- [5] Leupold J, *et al.*, *MRM* 55:557-65, 2006.
- [6] Han F, *et al.*, *Proc 21st ISMRM*, p. 485, 2013.
- [7] Luo J, *et al.*, *Proc 21st ISMRM*, p. 2581, 2013.
- [8] Santos JM, *et al.*, *Conf Proc IEEE Eng Med Biol Soc* 2:1048-51, 2004.